High Density RF MIM Capacitors Using High-κ $AlTaO_x$ Dielectrics

C. H. Huang [a], M.Y. Yang [a], Albert Chin [a], Chunxiang Zhu [b], M. F. Li [b], and Dim-Lee Kwong [c]

[a] Dept. of Electronics Eng., National Chiao Tung Univ., Hsinchu, Taiwan
[b] Silicon Nano Device Lab, Dept. of Electrical and Computer Engineering, National Univ. of Singapore, Singapore, 119260
[c] Dept. of Electrical & Computer Eng., The Univ. of Texas, Austin, TX 78752, USA

Abstract — **Very high capacitance density of 10 fF/μm² is measured using high-κ $AlTaO_x$, with small capacitance reduction of 5% from 10 KHz to 30 GHz, low loss tangent < 0.03, and process compatible with existing VLSI back-end integration. Small voltage dependence of capacitance < 600 ppm, mathematical derived from S-parameters, is obtained at 1 GHz, which ensures this MIM capacitor useful for high precision circuits operated at RF regime.**

I. INTRODUCTION

The RF MIM capacitor is widely used for impedance matching and filtering, but the total capacitor area usually consumes a large portion of the whole chip size. According to International Technology Roadmap for Semiconductors (ITRS) [1], the continuously increasing MIM capacitor density is required to reduce chip area and cost. The method to achieve higher capacitance density ($\varepsilon_0\kappa/t_d$) is to use high-κ gate dielectric [2]-[6], because the decreasing dielectric thickness (t_d) will largely increase the undesired leakage current and loss tangent. Therefore, the primary technology challenge for high density MIM capacitor is to search suitable high-κ dielectric with good dielectric integrity when fabricated at a low process temperature ≤ 400°C for VLSI back-end process integration [3]-[6]. Another difficult challenge for RF MIM capacitor is to achieve small voltage dependence of capacitance (ΔC/C), or equivalently the quadratic voltage coefficient [1], [3] used for precision circuit application. In addition, it is highly desired to develop a method to measure the ΔC/C at RF frequency beyond the 1 MHz limitation of conventional precision LCR meter. This is because the operation speed of precision circuits is increasing into GHz range as continuous technology evolution. Previously, we have reported a relatively high MIM capacitance density of 5 fF/μm² using high-κ Al_2O_3 dielectric [5] and good RF performance is obtained [6]. However, the adding Ti and achieved higher κ and capacitance density is not useful for RF application due to fast capacitance reduction at high frequencies [6]. In this paper, we have successfully increased the capacitance density to 10 fF/μm² using higher-κ $AlTaO_x$ dielectric with good RF performance of weak capacitor reduction (5%) from 10 KHz to 30 GHz. Besides, a very small ΔC/C < 600 ppm (quadratic voltage coefficient of only 130 ppm/V^2) at RF frequency regime is obtained, using our mathematically derived ΔC/C from measured S-parameters. This small value is close to the future (year 2013) technology requirement of ITRS roadmap [1], which ensures this $AlTaO_x$ MIM capacitor technology useful in high speed precision circuits at RF regime.

II. EXPERIMENTAL PROCEDURE

Standard 4-in p-type Si wafers were used in this study. After grown 500 nm isolation SiO_2 from VLSI back-end process integration, the bottom capacitor electrode and GSG coplanar transmission line [6] were fabricated on SiO_2/Si substrates using deposited Pt/Ti bi-layer and patterning. Then thin Al:Ta (1:6) layer was deposited on bottom Pt/Ti transmission line, followed by subsequent oxidation and annealing at 400°C to form high-κ $AlTaO_x$ dielectric. This 400°C low temperature is due to the VLSI backend process integration limitation. Two $AlTaO_x$ thicknesses of 16 and 21 nm are formed. The motivation of choosing $AlTaO_x$ is to use higher κ property of TaO_x and preserves the merit of good RF MIM capacitor integrity using Al_2O_3 dielectric [3], [5]. Finally, Al metal was deposited and patterned for both top capacitor electrode and transmission line with capacitor area of 50 μm×50 μm. The $AlTaO_x$ MIM capacitors were characterized using HP4284A precision LCR meter from 10 KHz to 1 MHz, and the S-parameters were measured by HP8510C network analyzer from 200 MHz to 30 GHz and de-embedded from a dummy device [6]-[10]. The high frequency capacitance was extracted using a physically based equivalent circuit model reported previously [6]. The RF frequency ΔC/C and quadratic voltage coefficient are derived mathematically from measured S-parameters and circuit theory.

III. RESULTS AND DISCUSSION

A. Low frequencies characteristics:

0-7803-7695-1/03/$17.00 © 2003 IEEE

Fig.1 shows the C-V characteristics for $AlTaO_x$ MIM capacitors with two different dielectric thicknesses. High capacitance density of 10.3 and 7.2 fF/μm² are measured at 100 KHz for respective 16 and 21 nm physical thickness that gives a κ value of 18 in $AlTaO_x$ dielectric.

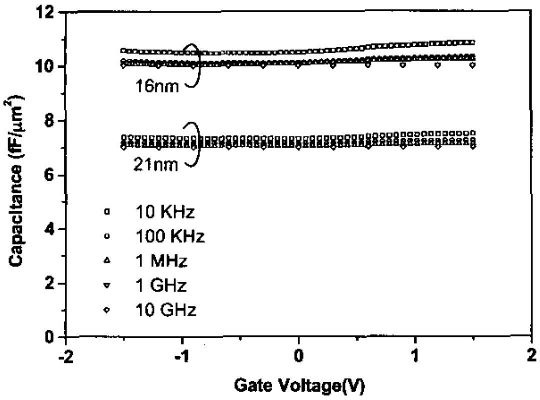

Fig. 1. C-V characteristics of the $AlTaO_x$ MIM capacitors measured at the frequencies from 10 KHz to 10 GHz. The 10 KHz to 1 MHz data is measured by precision LCR meter and the capacitance data >1 MHz is extracted from S-parameters.

Fig. 2 shows the J-V characteristics of $AlTaO_x$ MIM capacitors. The leakage current increases with decreasing the $AlTaO_x$ thickness, by trading off the increasing capacitance density. The asymmetrical J-V and slightly higher leakage current at positive voltage is due to the smaller work function of top Al than bottom Pt electrode. Electrons can be easier injected from Al electrode than larger work function Pt to give a higher leakage current. Leakage currents of 4.4×10^{-7} and 3.6×10^{-6} A/cm² are measured at -1V that is much better than the previous $AlTiO_x$ MIM capacitor [5] and suitable for RF circuit.

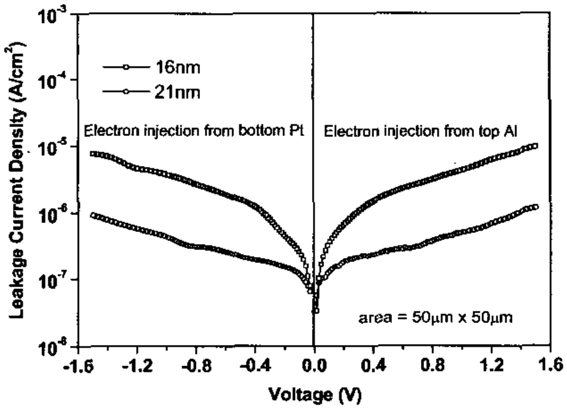

Fig. 2. J-V characteristics of $AlTaO_x$ MIM capacitors.

Figs. 3(a) and 3(b) show the ΔC/C characteristics for $AlTaO_x$ MIM capacitors, with physical thickness of 16 and 21 nm respectively. The ΔC/C below 1 MHz is obtained from the C-V measurement in Fig. 1. The using Al electrode (+V bias) gives poorer ΔC/C than Pt (-V bias), which has the same trend as higher leakage current shown in Fig. 2. The ΔC/C also becomes worse for thinner $AlTaO_x$ thickness. The decreasing ΔC/C in Fig. 3 and capacitance value in Fig. 1 with increasing frequency suggest the mechanism may be defect-related, since the traps may not have enough speed to follow the high frequency signals [8]-[9].

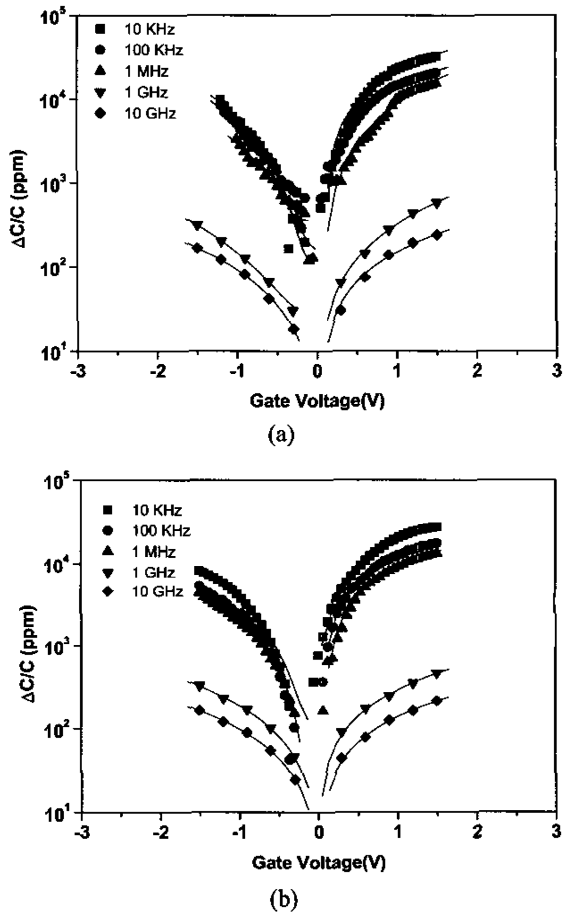

Fig. 3. Voltage dependence of capacitance ΔC/C for the MIM $AlTaO_x$ capacitors with dielectric thickness of (a)16 nm and (b) 21 nm. The 10 KHz to 1 MHz data is from the C-V measurement in Fig. 1, and the ΔC/C data >1 MHz is mathematically derived from S-parameters using circuit theory in equation (1) to (3).

B. High frequencies characteristics:

To further study the ΔC/C and other high frequency characteristics beyond the measurement capability of precision LCR meter, we have measured the S-parameters up to 30 GHz. Figs. 4(a) and 4(b) show the measured and modeled S-parameters for $AlTaO_x$ MIM capacitors, with 16 and 21 nm dielectric thickness respectively. The modeled S-parameter is from the physically based equivalent circuit [6] shown in Fig. 5, where R_S, L_S, R_P, and C are the parasitic series resistance, parasitic series inductance, parallel resistance, and the capacitor, respectively. The R_S and L_S are physically from transmission lines. Good agreement between measured and modeled S-parameters is obtained over the entire frequency range from 200 MHz to 30 GHz for $AlTaO_x$ MIM capacitors with two different dielectric thicknesses. This indicates the good accuracy of the physically based model and can be used to extract capacitance value at RF frequencies. The derived ΔC/C at RF frequency is shown in (1), where Z(C) in (2) is the total impedance in the equivalent circuit model of Fig. 5 and Z_0 is the characteristic impedance of transmission line. The RF frequency ΔC/C in (1) is obtained by differentiating the measured S_{21} in (3), which shows the relation between S_{21} and total impedance Z(C).

$$\frac{\Delta C}{C} = \frac{Z_0\left(2+Z(C)/Z_0\right)^2}{2R_P^2} j\omega C \left(R_P + 1/j\omega C\right)^2 \Delta(S_{21}) \qquad (1)$$

$$Z(C) = R_S + j\omega\left(L_{S1} + L_{S2}\right) + \frac{R_P / j\omega C}{R_P + 1/j\omega C} \qquad (2)$$

$$S_{21} = \frac{2}{2 + Z(C)/Z_0} \qquad (3)$$

The derived ΔC/C at 1 and 10 GHz are also plotted in Figs. 3(a) and 3(b) for two different dielectric thicknesses. The ΔC/C decreases with frequency increasing from 1 GHz to 10 GHz, which is consistent with the decreasing trend from 10 KHz to 1 MHz measured by precision LCR meter. This small ΔC/C < 600 ppm at 1 GHz or equivalent to a voltage coefficient of only 130 ppm/V^2 is close the future technology requirement for year 2013, according to of ITRS roadmap [1]. This excellent result indicates that the high-κ $AlTaO_x$ can be useful for high precision MIM capacitor and circuits at RF regime.

We have further plotted the extracted capacitance in Fig. 6 from the measured and simulated C-V data and S-parameters. Capacitance reduction of 5% is obtained for $AlTaO_x$ MIM capacitor over the entire frequency range from 10 KHz to 30 GHz. The slightly larger capacitance reduction is observed at thinner $AlTaO_x$, which may be due to slightly higher defect density with slow trap time constant at thinner thickness.

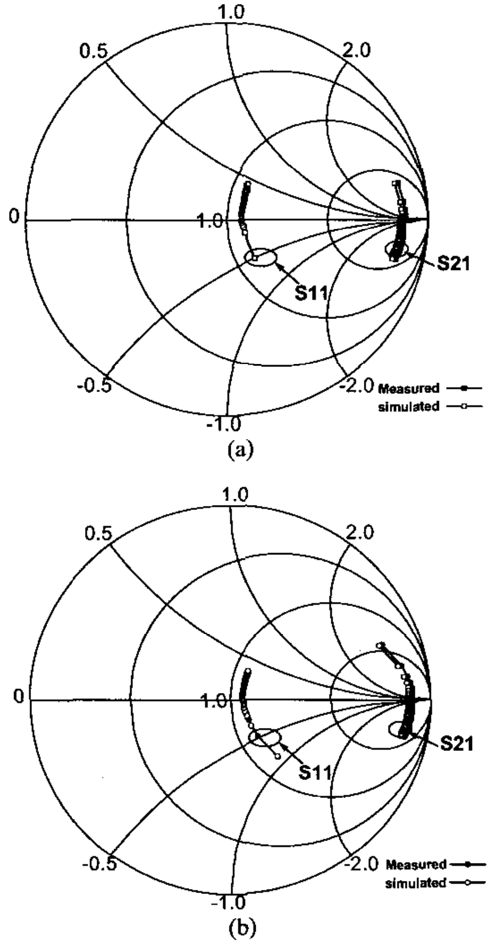

Fig. 4. The measured and simulated scattering parameters of $AlTaO_x$ MIM capacitors with the dielectric thickness of (a) 16 nm and (b) 21 nm. The measured frequency is ranged from 200 MHZ to 30 GHz. Good matching between measured and modeled data indicates the good accuracy of equivalent circuit in following figure.

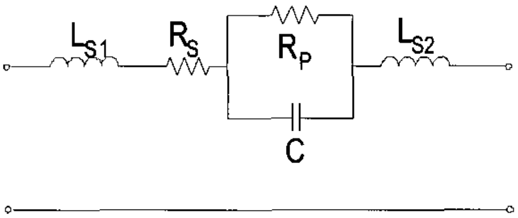

Fig. 5. The equivalent circuit model for capacitor simulation at RF regime. The R_S and L_S are the parasitic resistance and inductance from transmission lines, where the R_P and C are the parallel resistance for capacitor C.

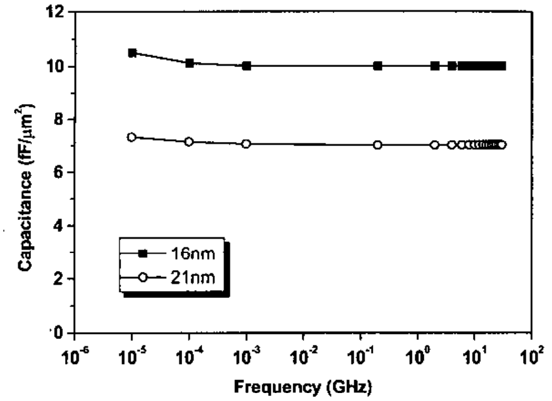

Fig. 6. The frequency-dependent capacitance for $AlTaO_x$ MIM capacitors with dielectric thickness of 16 and 21 nm. Small capacitance reduction shows the excellent device performance.

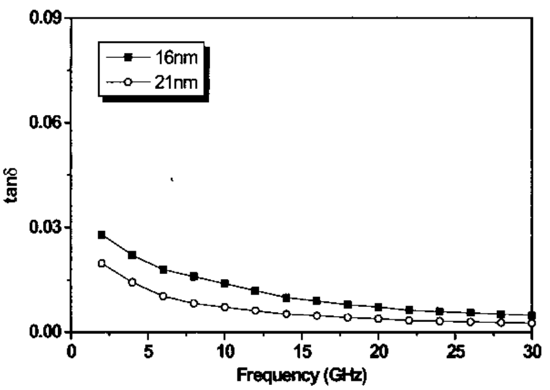

Fig. 7. The frequency-dependent loss tangent for $AlTaO_x$ MIM capacitors with thickness of 16 and 21 nm. The small loss tangent less than 0.03 suggests the good capacitor performance.

We have also plotted the loss tangent from the measured and simulated C-V and S-parameters. Fig. 7 shows the loss tangent for $AlTaO_x$ MIM capacitors. Good RF performance can be evidenced from the low loss tangent for both dielectric thicknesses. However, the loss tangent for 16 nm $AlTaO_x$ capacitor is slightly higher than that for 21 nm $AlTaO_x$ device, which is due to the larger leakage current and smaller R_P. The small capacitance reduction, high capacitance density, low loss tangent, and small $\Delta C/C$ < 600 ppm meet all the performance requirement of RF MIM capacitors.

V. CONCLUSION

We have achieved very high capacitance density of 10 fF/μm^2, small capacitance reduction of 5%, and small $\Delta C/C$ < 600 ppm at 1 GHz using high-κ $AlTaO_x$ processed at 400^{o}C. This good MIM capacitor integrity is suitable for precision circuit application at RF frequencies.

ACKNOWLEDGEMENT

This work has been sponsored by NSC (90-2215-E-009-044) and NSTB/EMT/TP/ 00/001.2.

REFERENCES

[1] International Technology Roadmap for Semiconductors, 2001 Edition, Process Integration, Devices, & Structure chapter, pp. 18-19.

[2] A. Chin, C. C. Liao, C. H. Lu, W. J. Chen, and C. Tsai, "Device and reliability of high-k Al_2O_3 gate dielectric with good mobility and low D_{it}," *Symp. on VLSI Technology Dig.*, 1999, pp. 133-134.

[3] H. Hu, C. Zhu, X. Yu, A. Chin, M. F. Li, B. J. Cho, and D. L. Kwong, "MIM Capacitors Using Atomic-Layer-Deposited High-κ $(HfO_2)_{1-x}(Al_2O_3)_x$ dielectrics," *IEEE Electron Device Lett.* 24, 2003.

[4] S. B. Chen, J. H. Chou, K. T. Chan, A. Chin, J. C. Hsieh, and J. Liu, "Frequency-dependent capacitance reduction in high-k $AlTiO_x$ and Al_2O_3 gate dielectrics from IF to RF frequency range," *IEEE Electron Device Lett.* 23, no. 4, pp. 203-205 (2002).

[5] S. B. Chen, J. H. Chou, A. Chin, J. C. Hsieh, and J. Liu, "High Density MIM Capacitors Using Al_2O_3 and $AlTiO_x$ Dielectrics," *IEEE Electron Device Lett.* 23, no. 4, pp. 185-187 (2002).

[6] S. B. Chen, J. H. Chou, A. Chin, J. C. Hsieh, and J. Liu, "RF MIM Capacitors Using High-K Al_2O_3 and $AlTiO_x$ Dielectrics," *IEEE MTT-S Int. Microwave Symp Dig.*, vol. 1, pp. 201-204, June 2002.

[7] K. T. Chan, A. Chin, C. M. Kwei, D. T. Shien, and W. J. Lin, "Transmission line noise from standard and proton-implanted Si," *IEEE MTT-S Int. Microwave Symp Dig.*, pp. 763-766, June 2001.

[8] K. T. Chan, A. Chin, Y. B. Chen, JuY.-D. Lin, D. T. S. Duh, and W. J. Lin, "Integrated antennas on Si, proton-implanted Si and Si-on-Quartz," *Int. Electron Devices Meetings (IEDM) Tech. Dig.*, pp. 903-906, 2001.

[9] Y. H. Wu, A. Chin, K. H. Shih, C. C. Wu, C. P. Liao, S. C. Pai, and C. C. Chi, "RF loss and crosstalk on extremely high resistivity (10k-1MΩ-cm) Si fabricated by ion implantation," *IEEE MTT-S Int. Microwave Symp. Dig.*, 2000, pp. 221-224.

[10] Y. H. Wu, A. Chin, C. S. Liang, and C. C. Wu, "The performance limiting factors as RF MOSFETs scale down," *IEEE RF IC Int. Microwave Symp. Dig.*, 2000, pp. 151-155.